Supporting Information for Mechanical Recycling of 3D Printed Thermosets for Reuse in Vat Photopolymerization

Erin M. Maines,[1] Michaela A. Polley,[2] Greg Haugstad,[3] Brenda Zhao,[1] Theresa M. Reineke,*[,4]

Christopher J. Ellison*[,1]

[1] Department of Chemical Engineering and Materials Science, University of Minnesota, Minneapolis, Minnesota 55455, United States

[2] Department of Chemistry and Department of Mathematics and Statistics, Carleton College, Northfield, Minnesota 55057, United States

[3] Characterization Facility, University of Minnesota, Minneapolis, Minnesota 55455, United States

[4] Department of Chemistry, University of Minnesota, Minneapolis, Minnesota 55455, United States

***Corresponding Authors:**

Christopher J. Ellison; Email: cellison@umn.edu

Theresa M. Reineke; Email: treineke@umn.edu

Table of Contents

Discussion: Batch-to-batch variation of the Formlabs clear resin

Three different batches of Formlabs clear resin were used throughout this paper. One clear resin batch (batch 1) was used for the film studies in **Table 1**, for the 3D printing studies, and the particle size analysis (**Figure S2**). Another batch (batch 2) was used to examine particle size differences under the microscope (**Figures S1** and **S3**) and the impact of large particles on the mechanical properties of films (**Table S2**). Finally, the last batch (batch 3) was used for the mixed material studies. The mechanical properties of this last batch with recycle content are shown in **Table S1**, indicating that the trends observed in **Table 1** are also present with this batch.

Table S1: Tensile test results from multiple recycling rounds using Formlabs Clear Resin (Batch 3).

Recycle Content (wt%)	Strain at Break (%)	Max Stress (MPa)	Modulus (GPa)	Toughness (MJ/m^3)	Number of samples
1st Recycling Round with Clear Resin					
0	8.07 ± 1.15	56.2 ± 1.9	1.16 ± 0.15	2.97 ± 0.69	3
10	6.41 ± 0.62	54.7 ± 6.0	1.27 ± 0.13	2.25 ± 0.46	3
2nd Recycling Round with Clear Resin					
10	8.43 ± 1.58	62.9 ± 4.1	1.13 ± 0.07	3.43 ± 1.03	5

Discussion: Particle size effects on mechanical properties

Previous studies on recycling crosslinked tire rubber found significant effects of the particle size of the ground tire rubber on the final mechanical properties in various systems.[1] For example, studies looking at either compressed ground tire rubber,[2,3] ground tire rubber dispersed in virgin rubber,[4,5] and ground tire rubber in polyolefins,[6,7] all found that large particles of ground tire rubber resulted in a decrease in the mechanical performance of the final materials. Therefore, understanding the particle size effects in the present system is important.

The clear resin was used for this study; however, the results are expected to translate to the other resin materials. The material was milled multiple times at fixed durations and imaged using an optical microscope after each milling cycle to understand the effect of milling time on particle size. It was observed that once the particles reached a size of around 100 μm (determined by optical microscopy), there was no further reduction in the particle size as a function of milling time (**Figure S1**). In all cases, this occurred after at least eight milling cycles. Therefore, each sample was milled for eight cycles to ensure the particle size was consistent across batches. This resulted in particles with a mean particle diameter (M_v) around 70 μm (**Figure S2A**). To determine the particle size effect on the mechanical properties, two different particle sizes were created, one considered large (determined by optical microscopy to be around 700 μm, **Figure S3A**) and one much smaller (around 100 μm, **Figure S3B**). These particles were mixed with neat liquid clear resin, cast into films, exposed to UV light, and tensile tested, following the path in the main manuscript **Figure 1A**. The material with large particles suffers from a 23% loss in strain at break and a 36% loss in maximum stress compared to the original neat material (**Table S2**). On the other hand, as shown in **Table S2**, the strain at break and maximum stresses for the material with small particle sizes are within error of the material without recycle content. This indicates that the larger particles create defects that cause the mechanical properties to deteriorate compared to the original material, similar to the studies conducted with ground tire rubber.[1–7] Overall, these film studies confirmed that large particles have an expected negative effect on mechanical properties, and longer milling times should be used to ensure smaller particles.

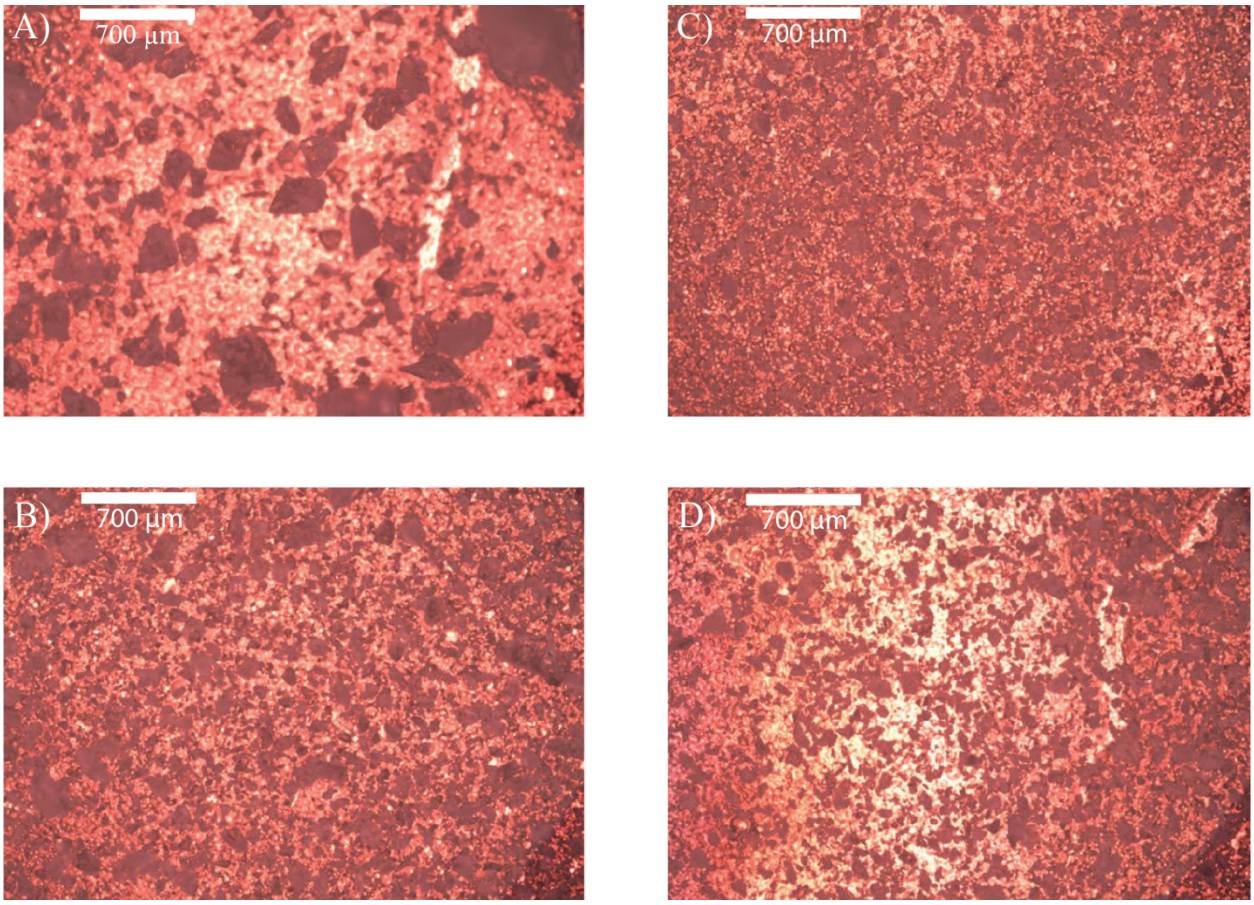

Figure S1: Optical microscope image demonstrating different particle sizes from Formlabs Clear Resin (batch 2). Two samples were milled and the particle size was imaged after the first milling cycle (A and C) and then after the second milling cycle (B and D). For the first set, after one milling cycle A) shows large particle sizes and after the second, B) the particle sizes decreased. For the second set, the particle size C) after one milling cycle was already small and so after a second milling cycle, D) there is little change in particle size.

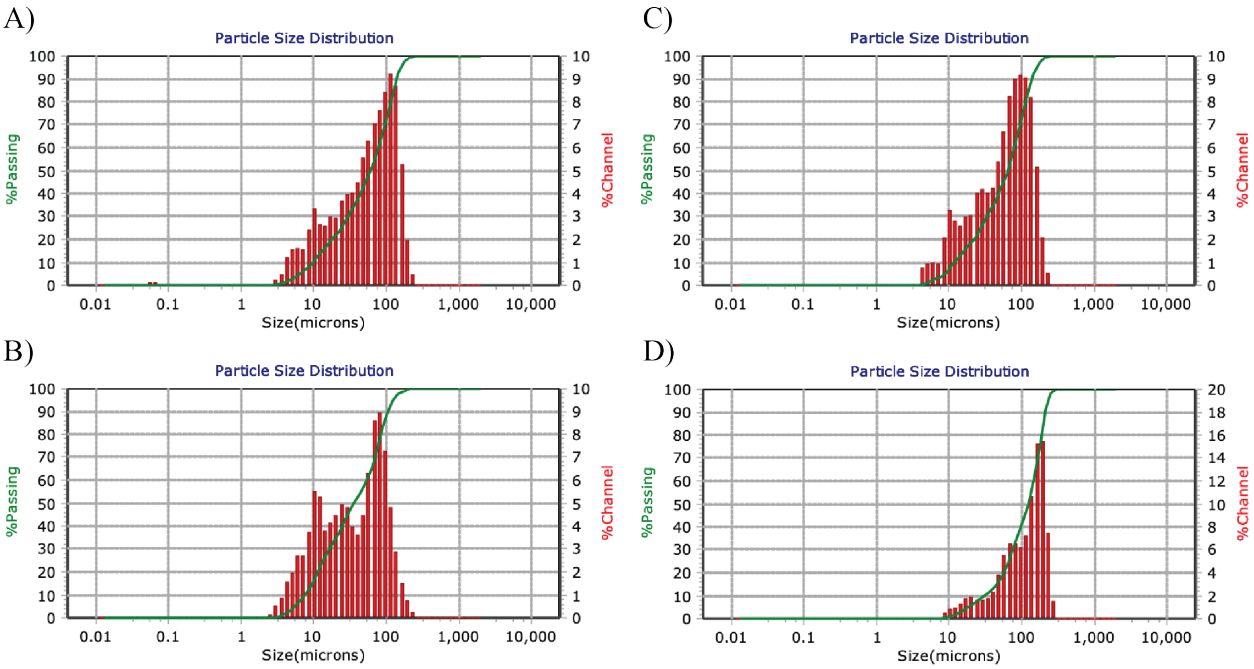

Figure S2: Particle size distribution determined by laser diffraction of A) Clear resin (batch 1) powder for films in **Table 1** with 10, 20, and 30 wt% recycle content with M_v = 68.5 μm. B) Clear resin powder for 2nd recycling round film in **Table 1** with M_v = 48.9 μm. C) Clear resin (batch 1) for 3D printing milled 8 cycles with M_v = 70.5 μm and D) Clear resin for 3D printing milled 2 cycles with M_v = 122 μm.

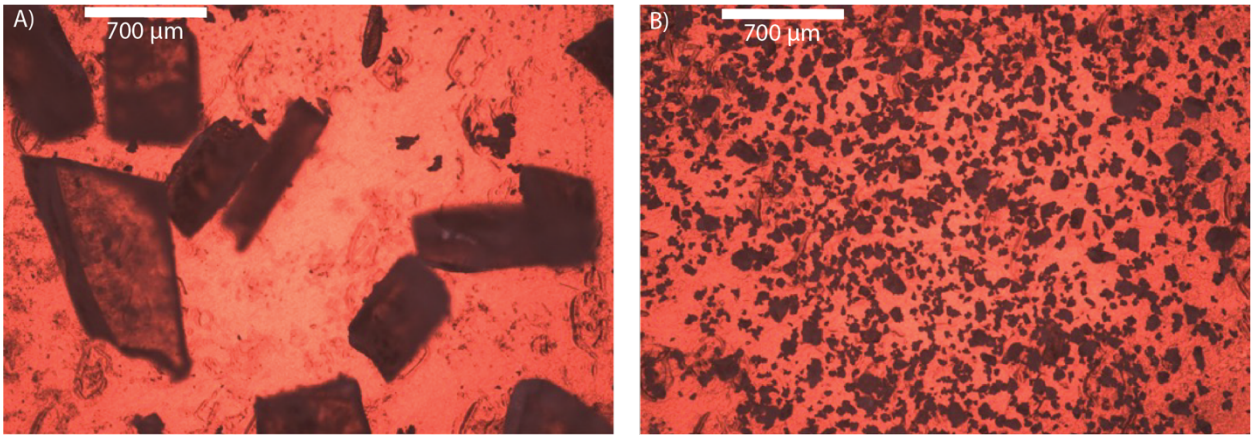

Figure S3: Optical microscope image demonstrating different particle sizes from the Formlabs Clear Resin (batch 2) where A) has large particle sizes and B) has been milled much longer to allow for smaller particle sizes.

Table S2: Tensile test results for films with Clear resin (batch 2) as a function of particle size.

Type of Particles (Batch 2)	Strain at Break (%)	Max Stress (MPa)	Modulus (GPa)	Toughness (MJ/m^3)	Number of samples
0 wt% Recycle Content					
N/A	5.47 ± 0.70	53.4 ± 6.0	1.26 ± 0.09	2.09 ± 0.85	3
20 wt% Recycle Content					
Large	4.20 ± 1.07	34.0* ± 7.9	0.95* ± 0.01	0.83 ± 0.36	3
Small	5.64 ± 2.82	56.6 ± 17.5	1.35 ± 0.07	2.57 ± 1.52	3

*Indicates the data point is statistically significant from two-sample t-test with a significance value of 0.05 compared to the original material with no recycle content

Discussion: Monomer diffusion as a function of time

Diffusion times for all the materials were examined to understand how long a soak time is needed for sufficient monomer swelling to produce an interpenetrating network, preventing the particles from acting as mechanical failure sites.

For the model monomer system, macroscopic swelling studies, as shown in **Figure S4,** indicated that the amount of liquid resin introduced into the network after 1 hour was similar to the amount at 24 hours. This suggested that shorter times would provide an increase in mechanical properties but still show network heterogeneity. To determine if the heterogeneity could be avoided, longer diffusion time scales beyond 24 hours were probed to determine if changes in monomer concentration would lead to a homogenous material over time. As an extreme condition, a sample was exposed to UV light after 14 days of diffusion time. DMA results on this sample still showed evidence of heterogeneity (**Figure S9**).

Similar macroscopic diffusion time studies were also investigated on both commercial materials (**Figure S4**), where the elastic network showed a significant increase in mass between 1

hour and 24 hours, which leveled off after 24 hours. On the other hand, the clear network was similar to the model material, with roughly the same amount of mass between 1 hour and 24 hours.

Recycled material formulations were prepared following the method depicted in **Figure 1A** to understand the effect of monomer absorption in the recycled particles on the final mechanical properties. For the elastic samples, liquid formulations with 5 wt% recycle content were mixed and then exposed to UV light at either 1 hour, 24 hours, or 48 hours post-mixing. The same procedure was conducted for the clear formulations at 10 wt% recycle content. The samples were then tensile tested to understand the effects of monomer diffusion on the final mechanical properties. As shown in **Figure S5 – S6**, little changes in strain at break and maximum stress were observed for either system as a function of time.

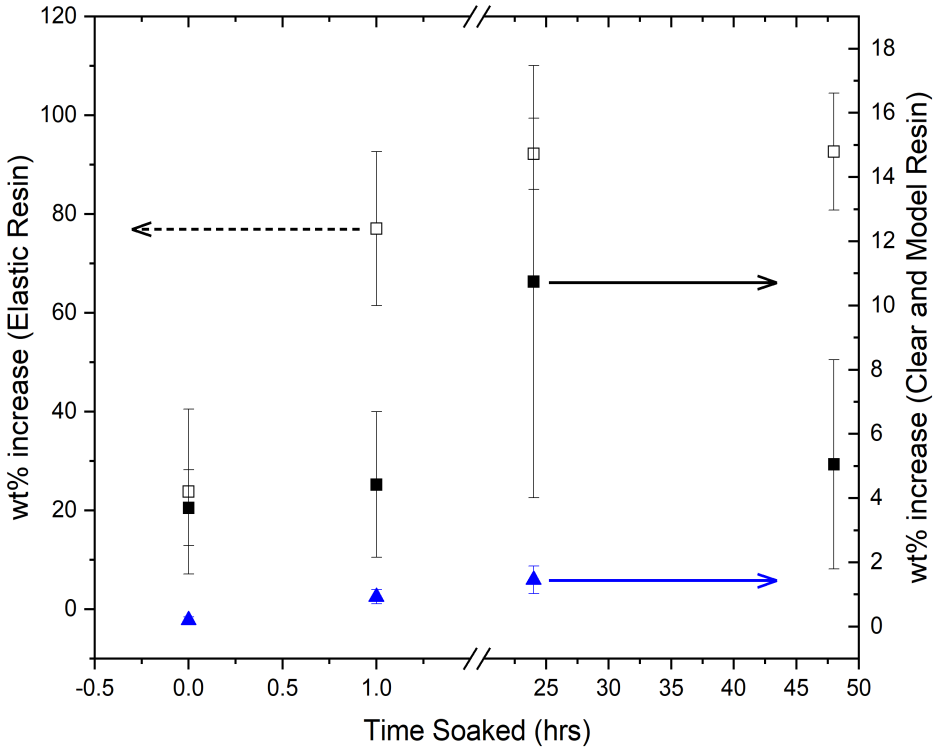

Figure S4: Weight percent increase of the network material (model, elastic, and clear) swelled in its own liquid monomer resin as a function of time. Note, the time zero point is to normalize for the resin left on the surface of the material and not swollen into the network.

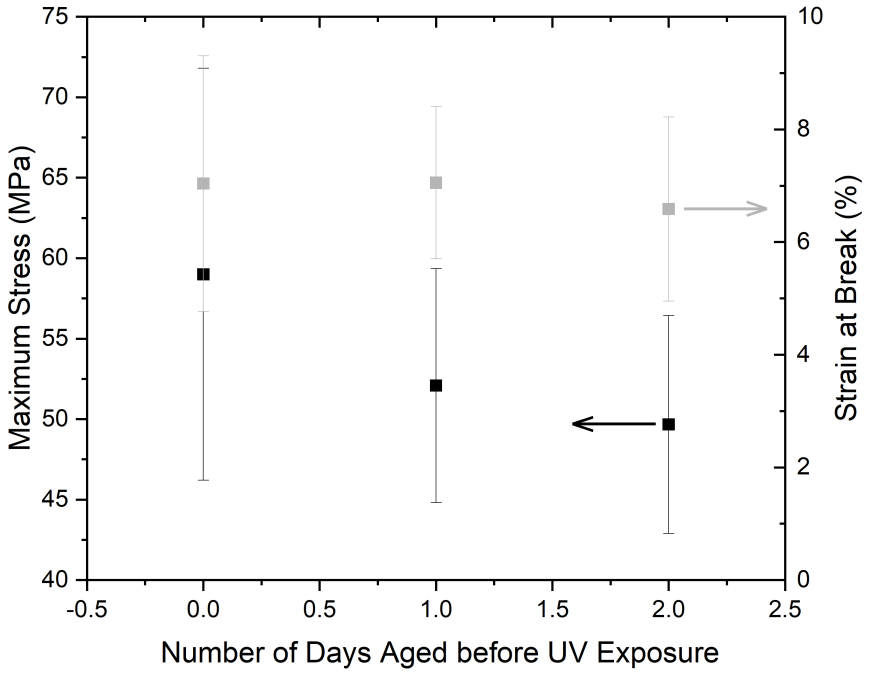

Figure S5: Average maximum stress (black squares) and strain at break (gray squares) for a clear matrix with 10 wt% clear recycle content where the formulation has been aged for 1 hour, 24 hours, and 48 hours prior to UV exposure.

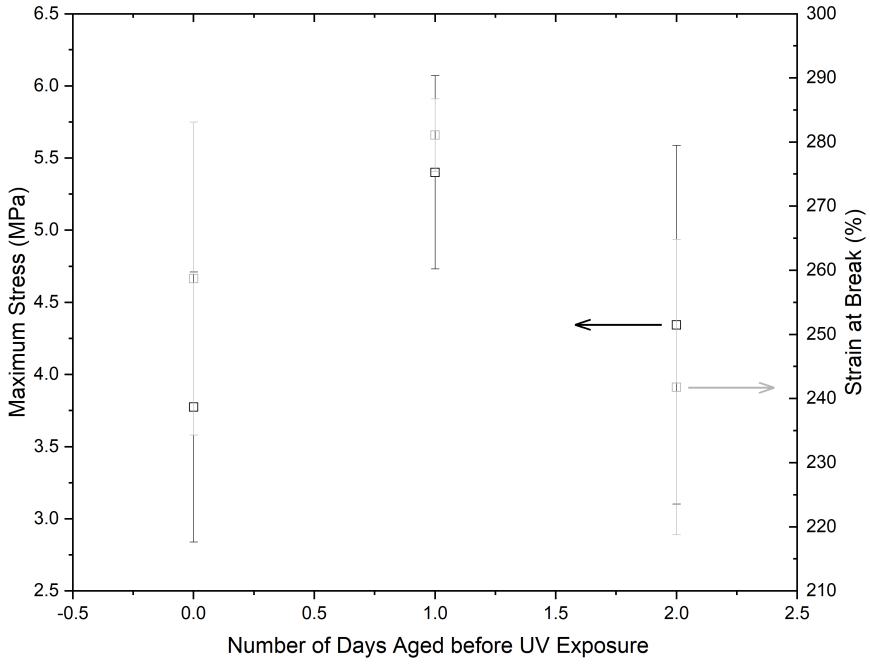

Figure S6: Average maximum stress (open black squares) and strain at break (open gray squares) for an elastic matrix with 5 wt% elastic recycle content where the formulation has been aged for 1 hour, 24 hours, and 48 hours prior to UV exposure.

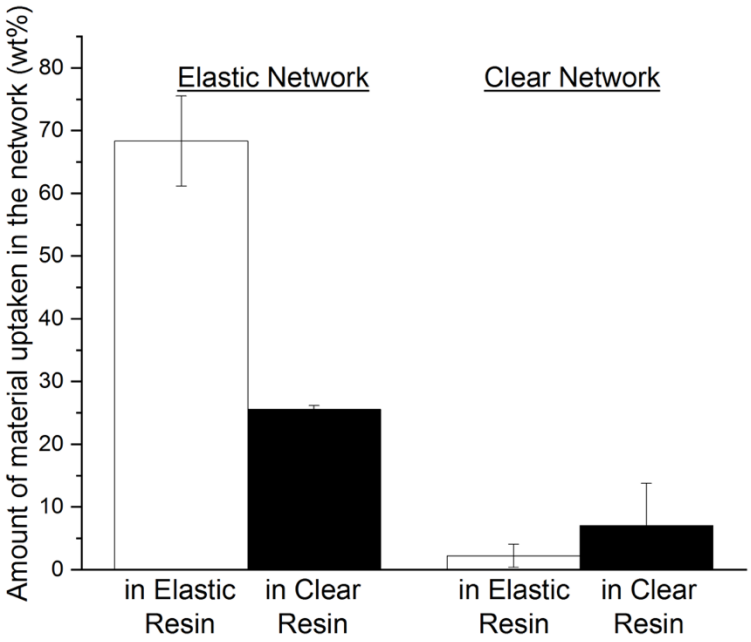

Figure S7: Swelling behavior of elastic and clear (batch 2) network material in its own monomer resin and the cross-monomer resin after soaking for 24 hours. These values are normalized to a material that was quickly dipped into the resin to account for any material left on the surface of the network.

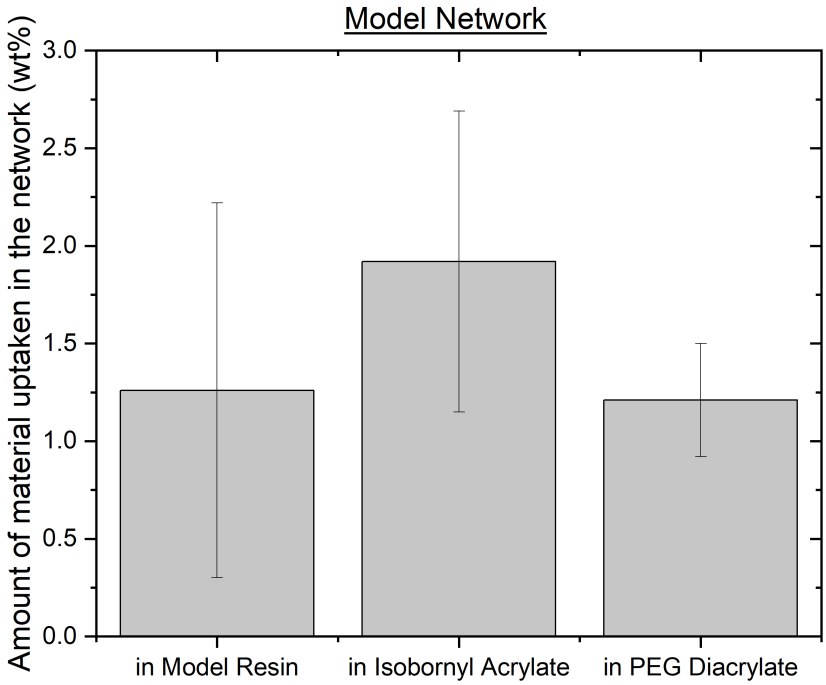

Figure S8: Swelling behavior of the model material in isobornyl acrylate, PEG diacrylate, and a 50/50 mixture of isobornyl acrylate and PEG diacrylate after 24 hours. These numbers are normalized to material that was quickly dipped into the resin to account for any monomer left on the surface of the network.

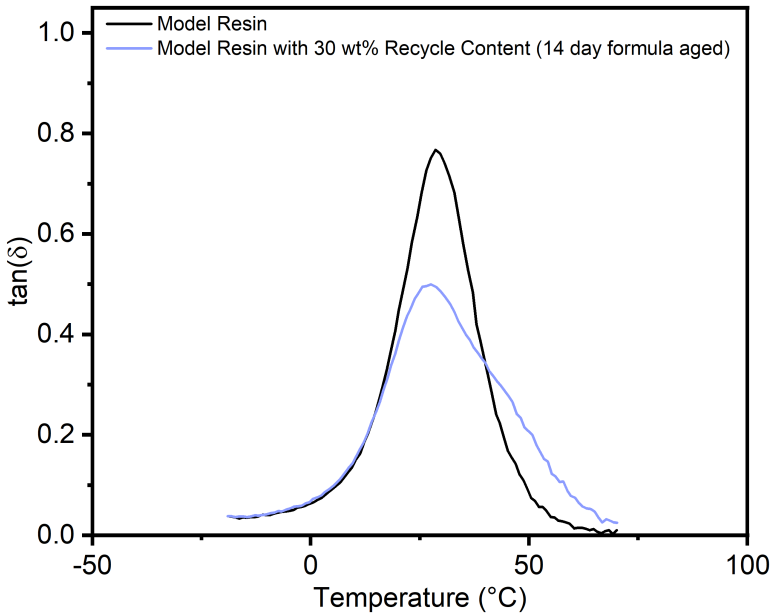

Figure S9: DMA tan(δ) as a function of temperature indicating heterogeneity (due to the multi-modal peak) in the model resin sample with 30 wt% recycle material even after 14 days of soaking.

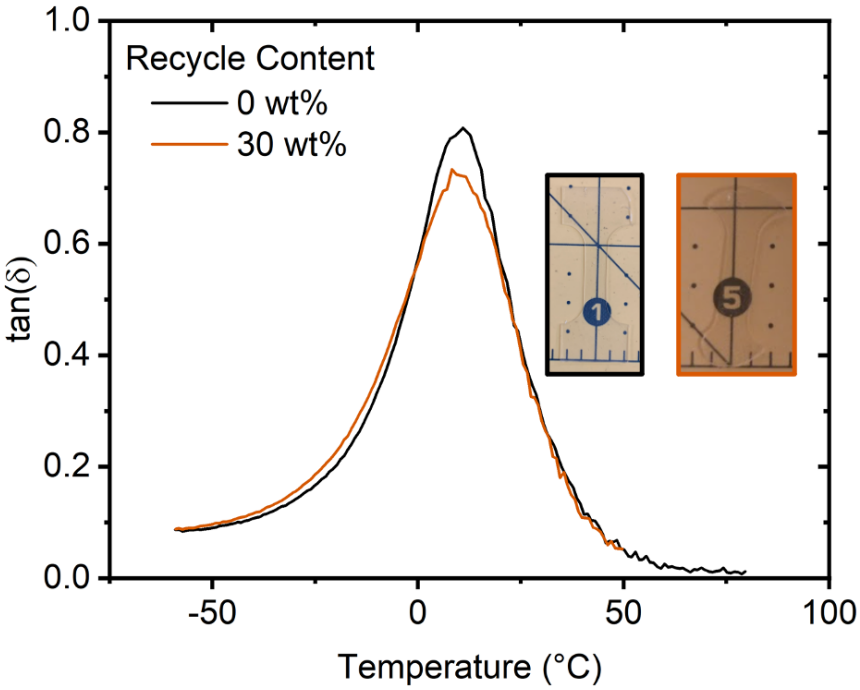

Figure S10: DMA tan(δ) data as a function of temperature in the Formlabs Elastic resin samples with and without recycle content.

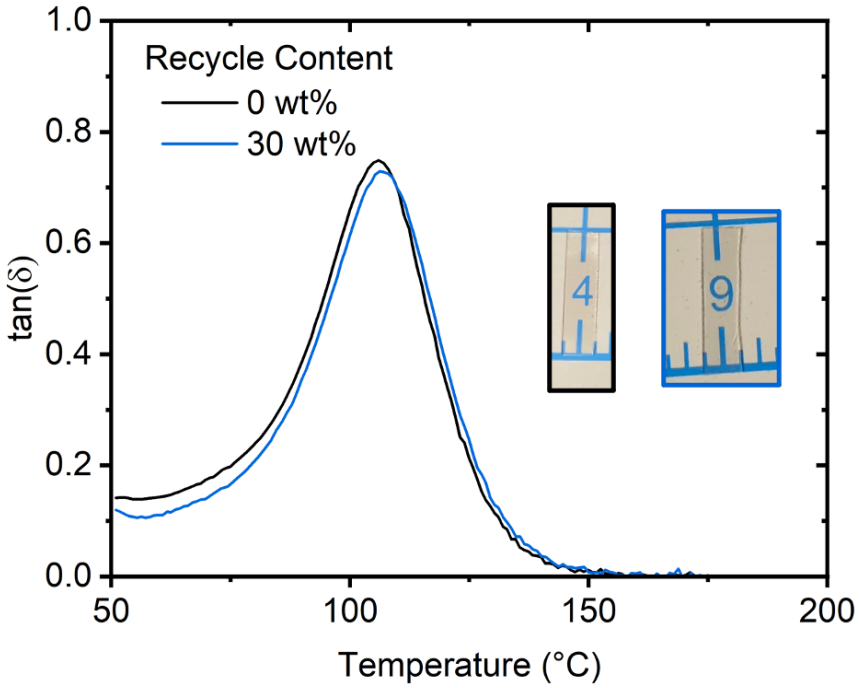

Figure S11: DMA tan(δ) data as a function of temperature in the Formlabs Clear resin (batch 1) samples with and without recycle content.

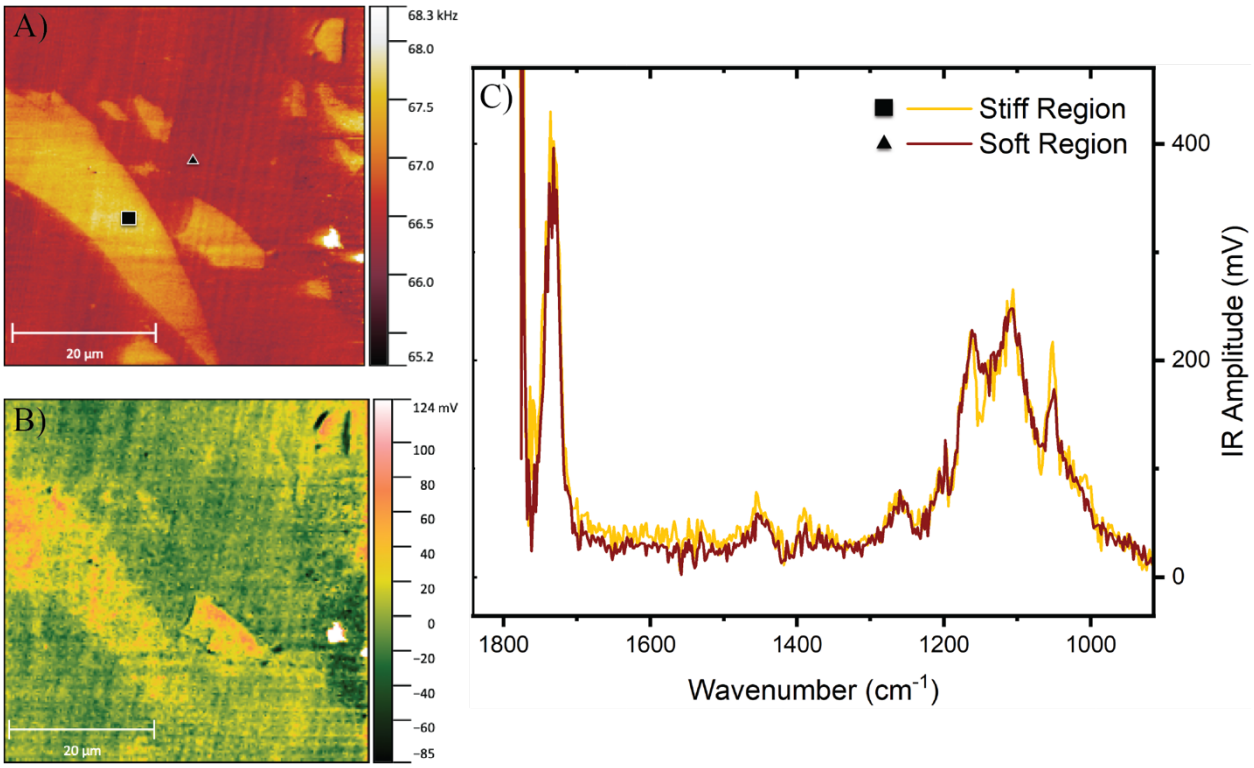

Figure S12: A) AFM-IR stiffness map of a model resin with 30 wt% recycle content. (Color scale is the contact resonance frequency, which is proportional to the square root of contact stiffness.) B) Corresponding IR absorbance image at 1100 cm^{-1}. (Color scale has been zeroed to the image average.) C) Wavenumber sweep of IR absorbance (gauged as contact resonance amplitude) at specific locations within a particle and the matrix. (The locations are indicated on the stiffness map with the matrix being represented with the triangle and the particles represented with the square.)

Table S3. Tensile test results as a function of recycle content for the model resin material.

Recycle Content (wt%)	Strain at Break (%)	Max Stress (MPa)	Modulus (GPa)	Toughness (MJ/m^3)	Number of samples
Resin Material: Model | Recycle Content: Model					
0	43.7 ± 5.4	6.43 ± 0.59	0.047 ± 0.005	1.65 ± 0.27	8
10	43.1 ± 4.4	7.47* ± 0.53	0.052 ± 0.008	1.92 ± 0.25	5
30	38.1 ± 5.5	8.19 ± 1.23	0.059* ± 0.005	2.01 ± 0.55	4

*Indicates the data point is statistically significant from two-sample t-test with a significance value of 0.05 compared to the original material with no recycle content

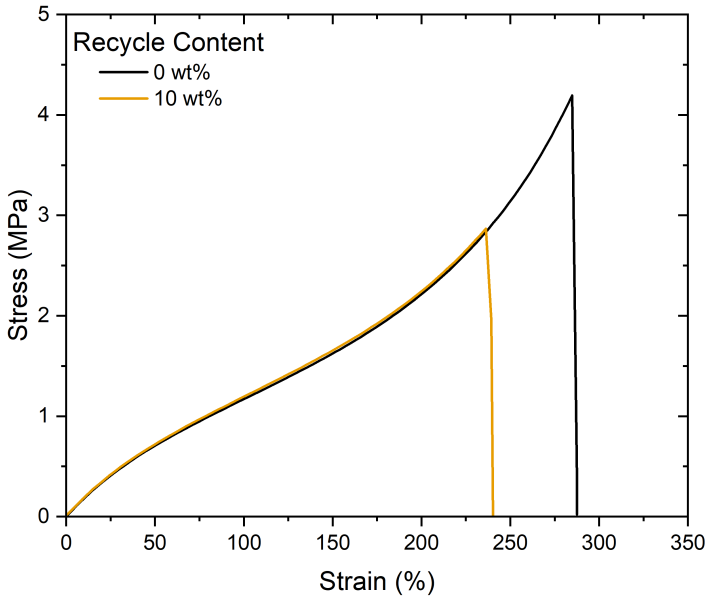

Figure S13: Representative stress-strain data for elastic resin material with and without recycle content.

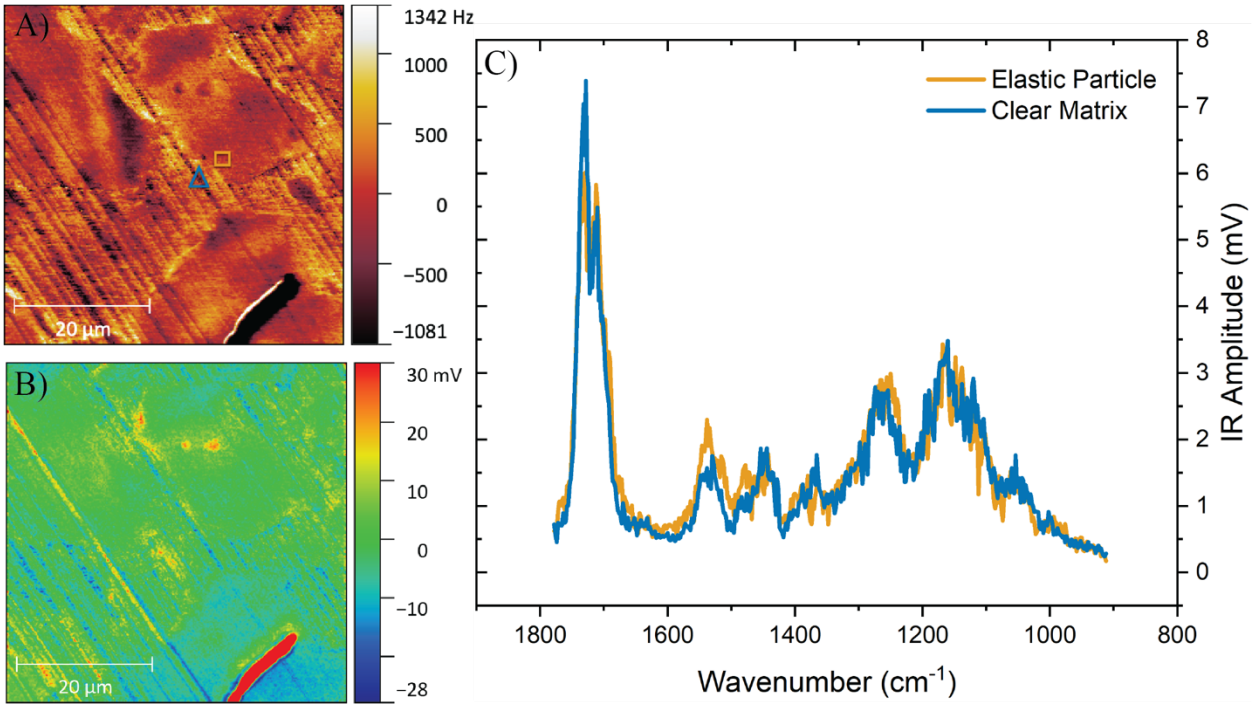

Figure S14: A) AFM-IR stiffness map of a clear (batch 3) matrix with 30 wt% elastic recycle content. B) Corresponding IR absorbance image at 1534 cm^{-1}. C) IR wavenumber sweep at specific locations within a particle and the matrix (the locations are indicated on the stiffness map with the matrix being represented with the blue triangle and the particles represented with the orange square).

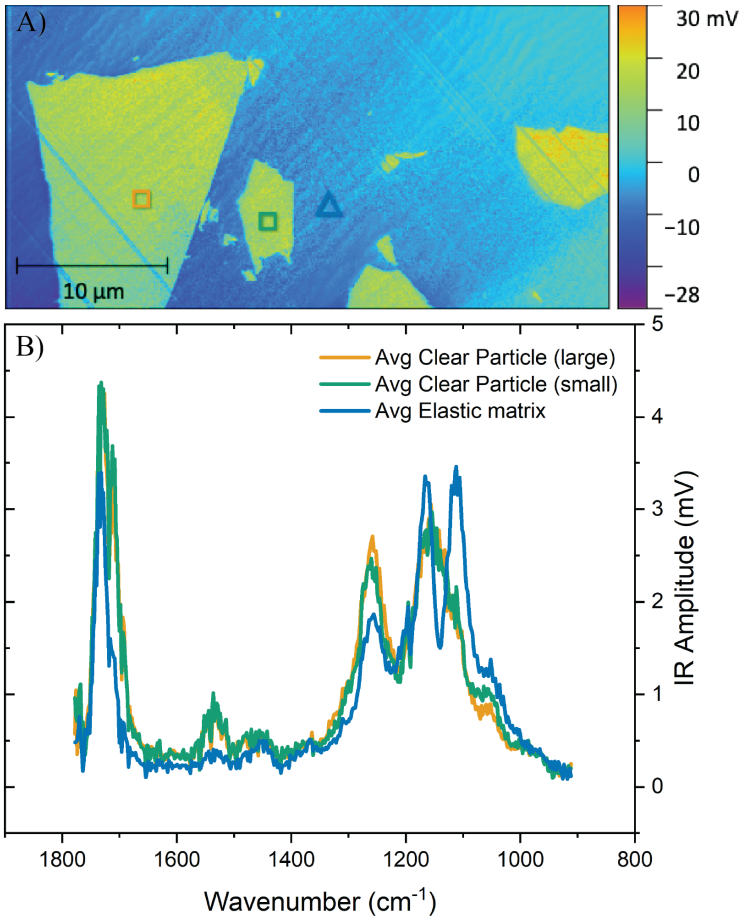

Figure S15: A) AFM-IR stiffness map at 1142 cm^{-1} of an elastic matrix with 30 wt% clear (batch 3) recycle content. B) Averaged IR spectra from specific regions within particle and matrix (locations indicated on the stiffness map, blue triangle being matrix and orange and green squares being particles).

Table S4: Tensile test data as a function of recycle content for the mixed materials where the matrix is clear and the recycle particles are elastic and the matrix is elastic and the recycle content is clear.

Recycle Content (wt%)	Strain at Break (%)	Max Stress (MPa)	Modulus (GPa)	Toughness (MJ/m^3)	Number of samples
Resin Material: Clear | Recycle Content: Elastic					
0	8.07 ± 1.15	56.2 ± 1.9	1.16 ± 0.15	2.97 ± 0.69	3
10	7.47 ± 1.30	48.9 ± 0.4	1.01 ± 0.05	2.38 ± 0.62	3
30	22.7 ± 7.1	28.0 ± 0.8	0.57 ± 0.02	5.56 ± 2.02	3
Resin Material: Elastic | Recycle Content: Clear					
0	285 ± 23	4.57 ± 1.16	0.0018 ± 0.0001	5.23 ± 1.25	8
10	151 ± 11	4.29 ± 0.72	0.0032 ± 0.0004	3.14 ± 0.71	3
30	72.2 ± 1.8	4.82 ± 0.41	0.0079 ± 0.0005	1.97 ± 0.25	3

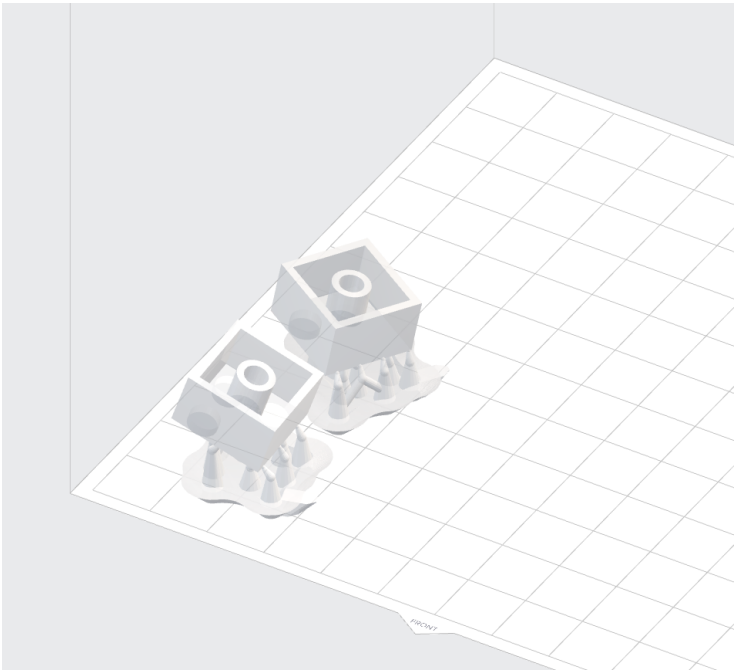

Figure S16: Image of Formlabs software print set up for the bricks.

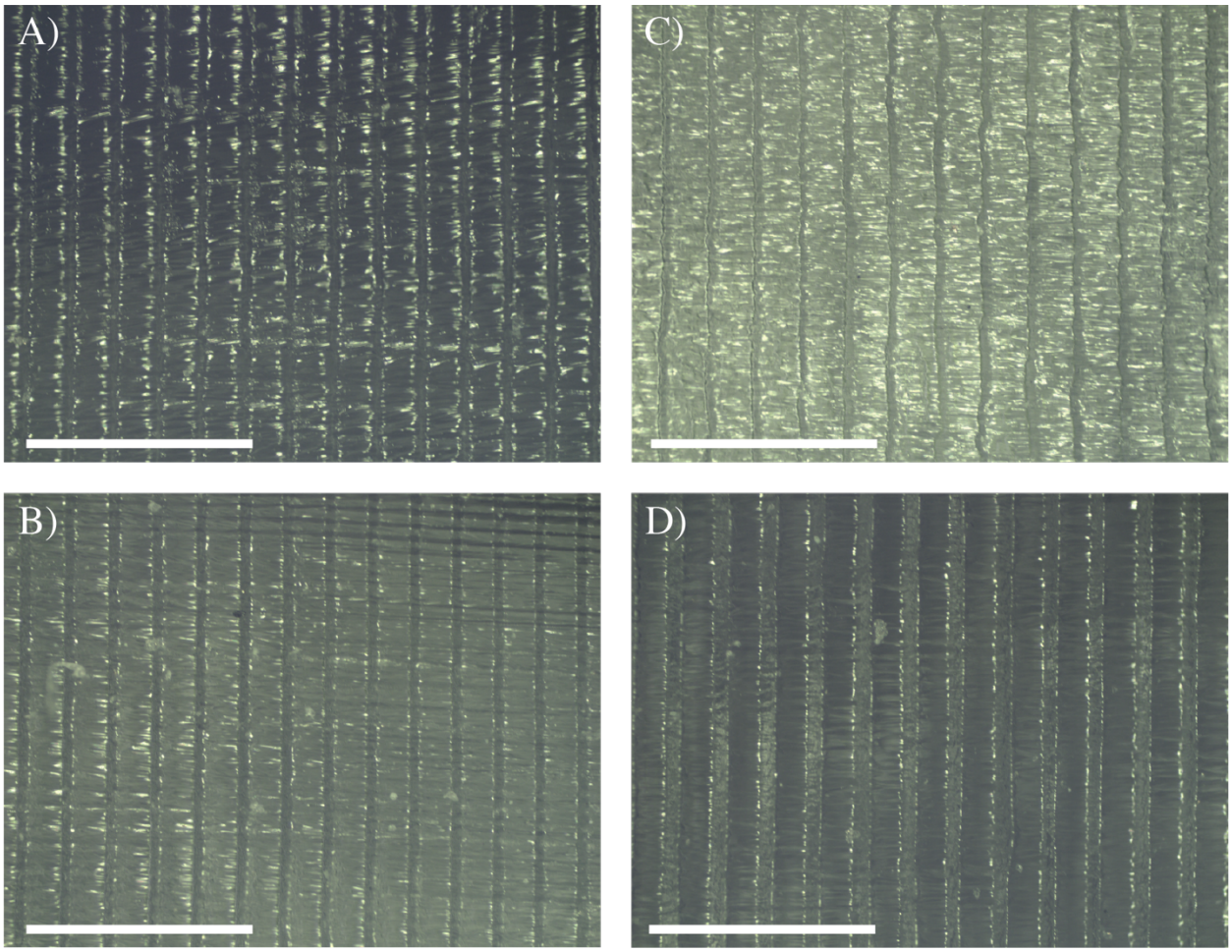

Figure S17: Microscope images of all four sides of a brick of Clear resin (batch 1) printed with 200 µm layer thickness. Layers are perpendicular to the 1000 µm scale bar (A-D). The horizontal lines in the images are due to the scanning laser path during printing.

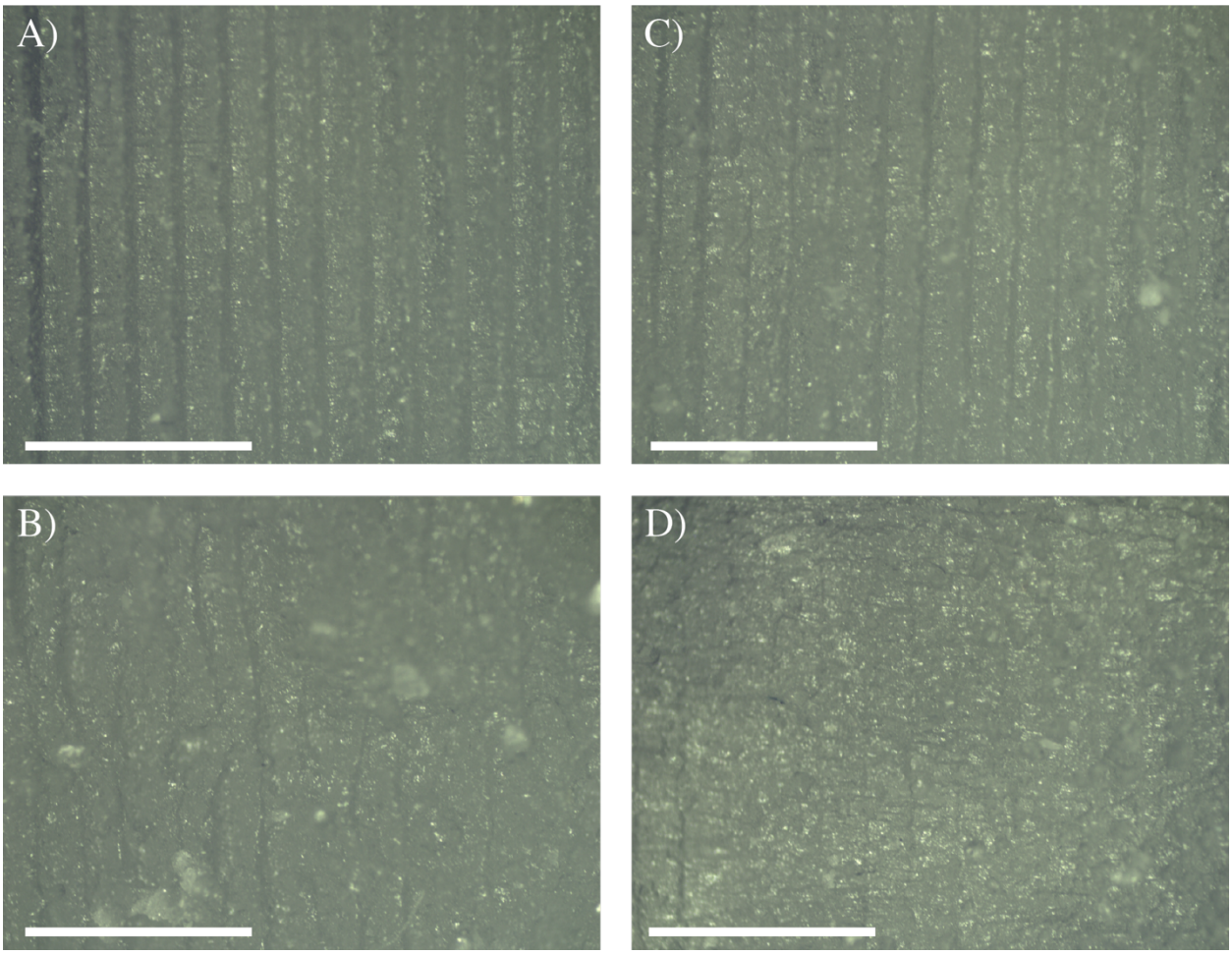

Figure S18: Microscope images of all four sides of a brick of Clear resin (batch 1) with 10 wt% recycle content (particle size of 70 µm) printed with 200 µm layer thickness. Layers are perpendicular to the 1000 µm scale bar (A-D). The horizontal lines in the images are due to the scanning laser path during printing.

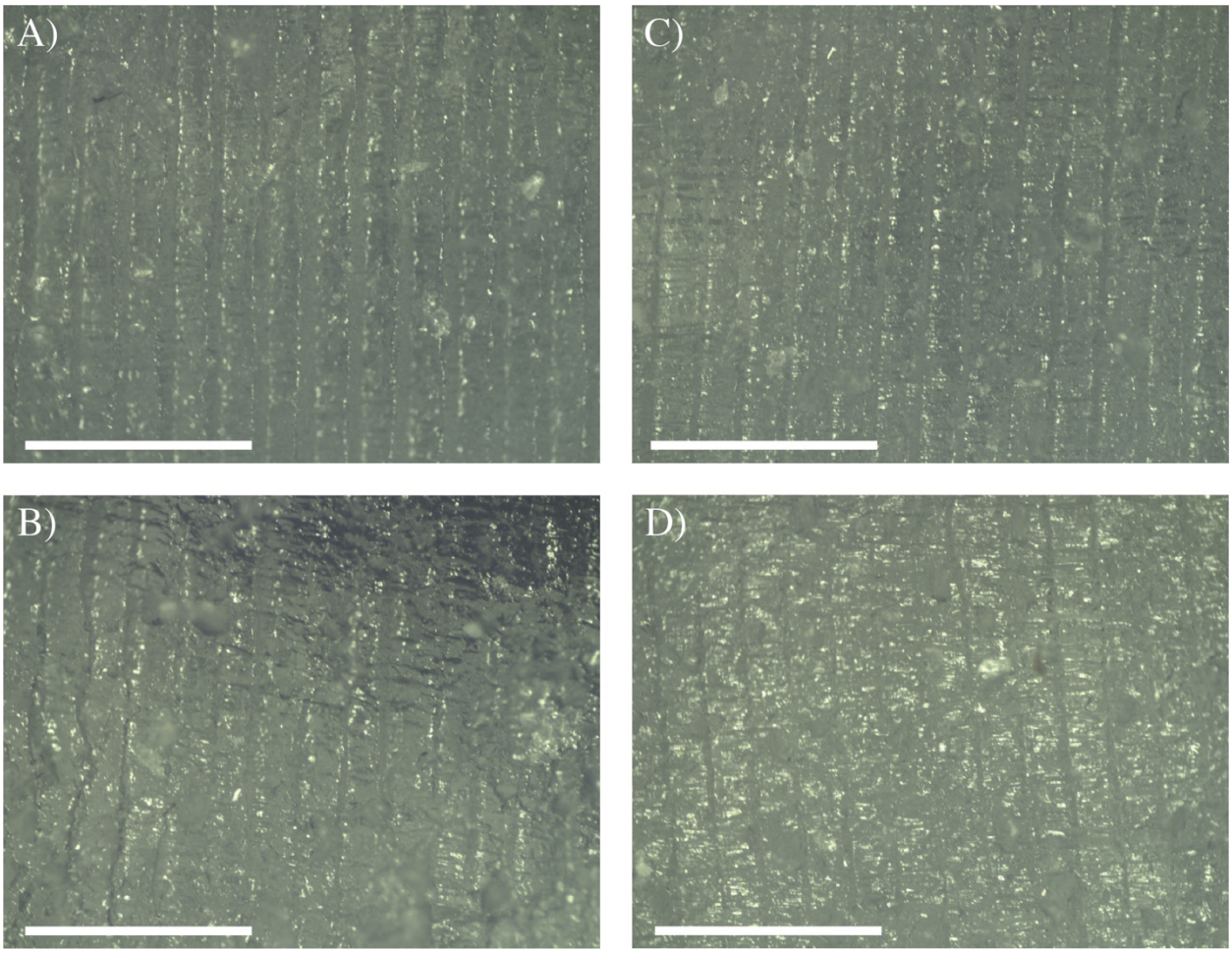

Figure S19: Microscope images of all four sides of a brick of Clear resin (batch 1) with 10 wt% recycle content (particle size of 122 µm) printed with 200 µm layer thickness. Layers are perpendicular to the 1000 µm scale bar (A-D). The horizontal lines in the images are due to the scanning laser path during printing.

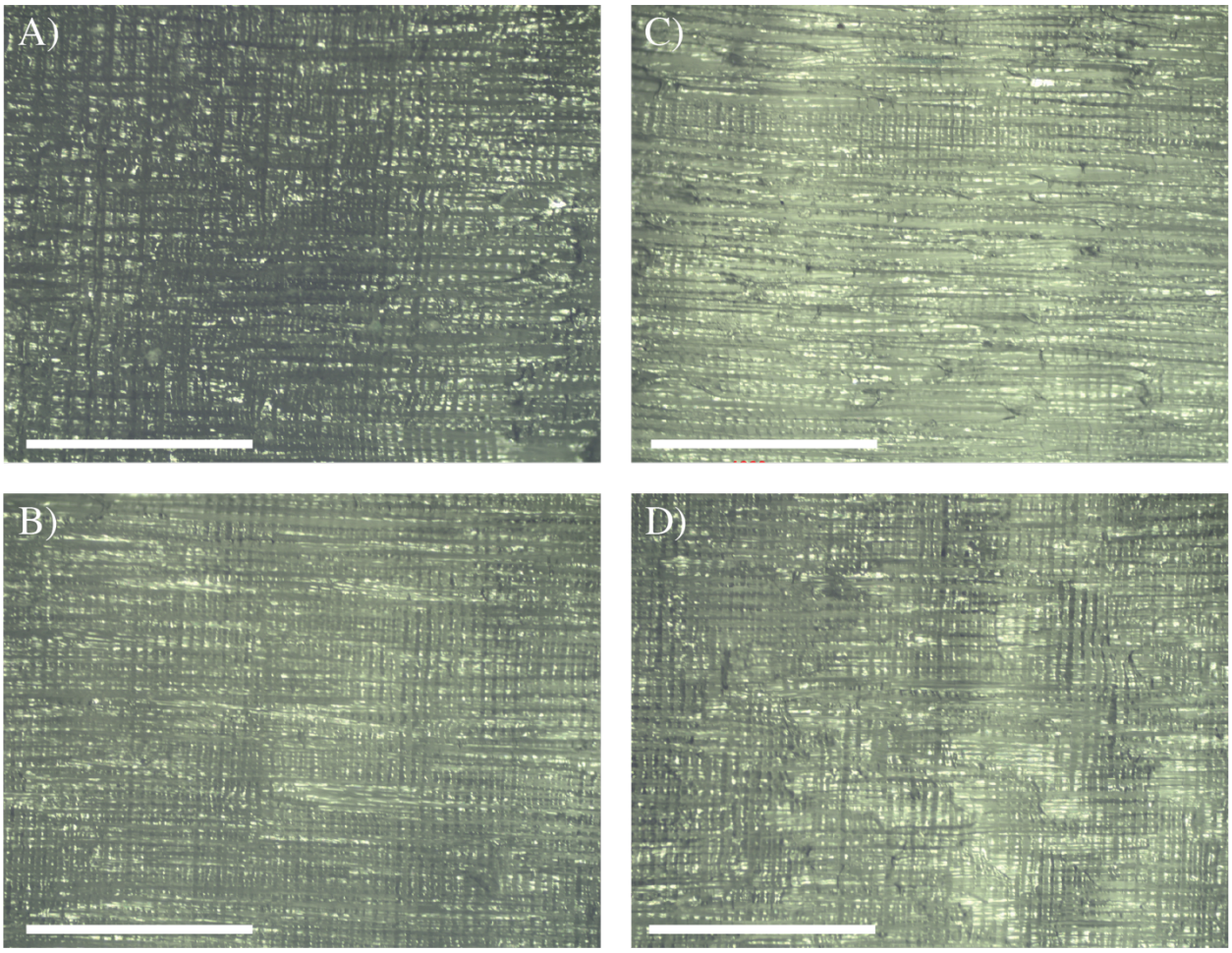

Figure S20: Microscope images of all four sides of a brick of Clear resin (batch 1) printed with 50 µm layer thickness. Layers are perpendicular to the 1000 µm scale bar (A-D). The horizontal lines in the images are due to the scanning laser path during printing.

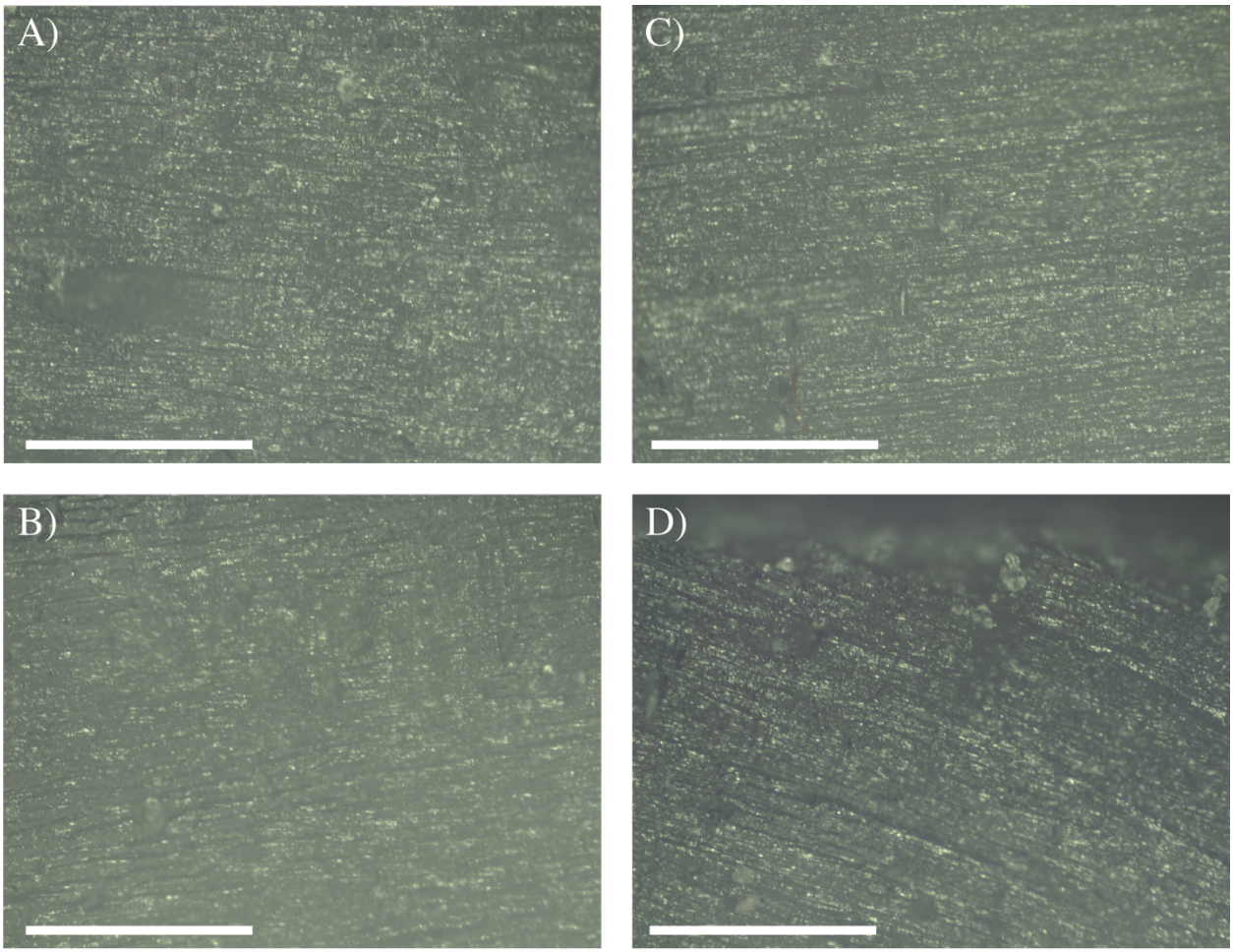

Figure S21: Microscope images of all four sides of a brick of Clear resin (batch 1) with 10 wt% recycle content (particle size of 70 µm) printed with 50 µm layer thickness. Layers are perpendicular to the 1000 µm scale bar (A-D). Note, the supports failed on one edge due to limited resin so in (D) the layers are sloped slightly to the right due to sag. The horizontal lines in the images are due to the scanning laser path during printing.

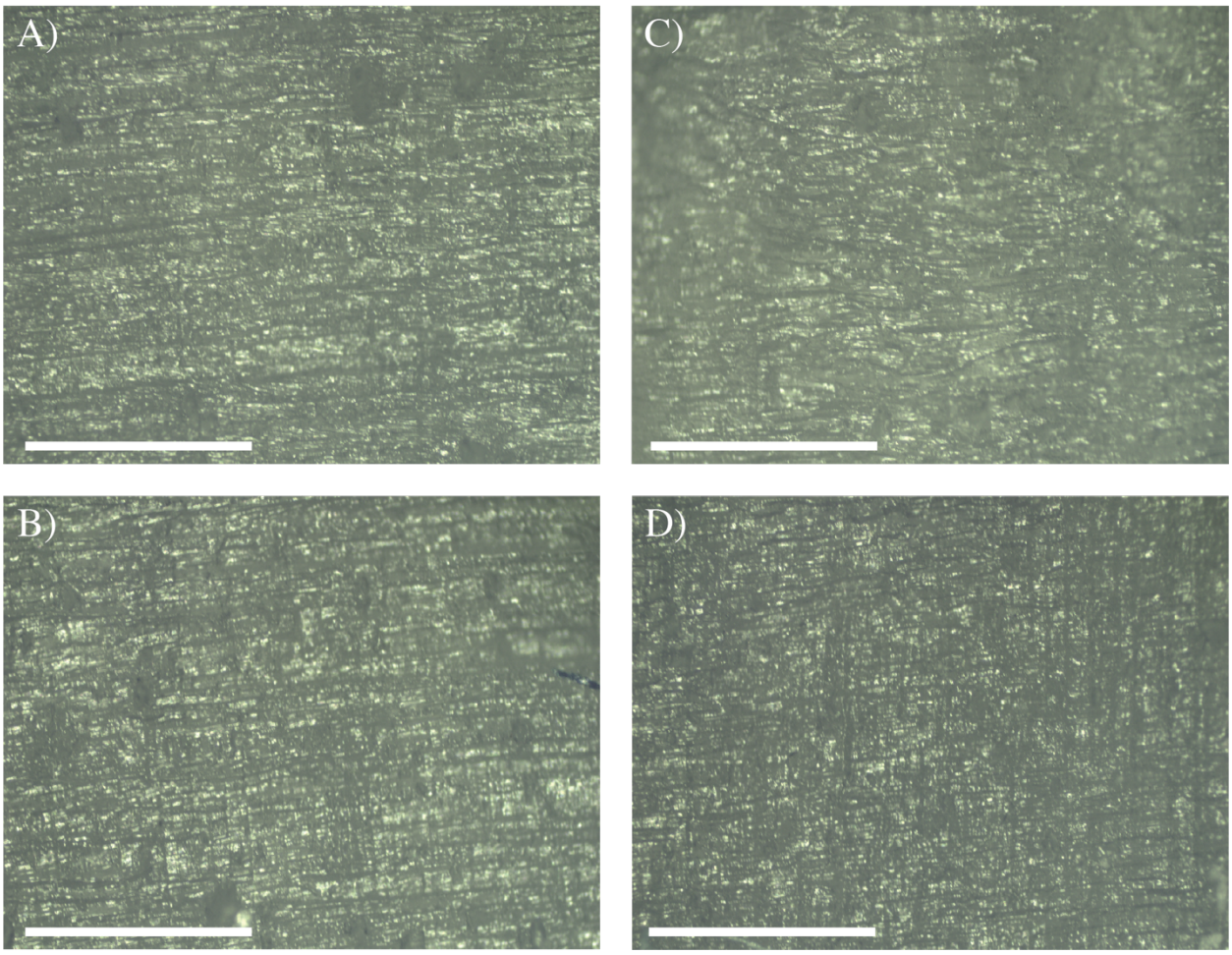

Figure S22: Microscope images of all four sides of a brick of Clear resin (batch 1) with 10 wt% recycle content (particle size of 122 µm) printed with 50 µm layer thickness. Layers are perpendicular to the 1000 µm scale bar (A-D). The horizontal lines in the images are due to the scanning laser path during printing.

References

(1) Karger-Kocsis, J.; Mészáros, L.; Bárány, T. Ground Tyre Rubber (GTR) in Thermoplastics, Thermosets, and Rubbers. *J. Mater. Sci.* **2013**, *48* (1), 1–38. https://doi.org/10.1007/s10853-012-6564-2.

(2) Gugliemotti, A.; Lucignano, C.; Quadrini, F. Production of Rubber Parts by Tyre Recycling without Using Virgin Materials. *Plast. Rubber Compos.* **2012**, *41* (1), 40–46. https://doi.org/10.1179/1743289811Y.0000000010.

(3) Bilgili, E.; Dybek, A.; Arastoopour, H.; Bernstein, B. A New Recycling Technology: Compression Molding of Pulverized Rubber Waste in the Absence of Virgin Rubber. *J. Elastomers Plast.* **2003**, *35* (3), 235–256. https://doi.org/10.1177/0095244303035003004.

(4) Han, S.-C.; Han, M.-H. Fracture Behavior of NR and SBR Vulcanizates Filled with Ground Rubber Having Uniform Particle Size. *J. Appl. Polym. Sci.* **2002**, *85* (12), 2491–2500. https://doi.org/10.1002/app.10575.

(5) Mathew, G.; Singh, R. .; Nair, N. .; Thomas, S. Recycling of Natural Rubber Latex Waste and Its Interaction in Epoxidised Natural Rubber. *Polymer* **2001**, *42* (5), 2137–2165. https://doi.org/10.1016/S0032-3861(00)00492-4.

(6) Colom, X.; Cañavate, J.; Carrillo, F.; Suñol, J. J. Effect of the Particle Size and Acid Pretreatments on Compatibility and Properties of Recycled HDPE Plastic Bottles Filled with Ground Tyre Powder. *J. Appl. Polym. Sci.* **2009**, *112* (4), 1882–1890. https://doi.org/10.1002/app.29611.

(7) Oliphant, K.; Baker, W. E. The Use of Cryogenically Ground Rubber Tires as a Filler in Polyolefin Blends. *Polym. Eng. Sci.* **1993**, *33* (3), 166–174. https://doi.org/10.1002/pen.760330307.